Cancer Letters 456 (2019) 59–68

Contents lists available at ScienceDirect

Cancer Letters

journal homepage: www.elsevier.com/locate/canlet

Original Articles

IGF1R/IRS1 targeting has cytotoxic activity and inhibits PI3K/AKT/mTOR and MAPK signaling in acute lymphoblastic leukemia cells

Ana Paula Nunes Rodrigues Alves[a], Jaqueline Cristina Fernandes[a], Bruna Alves Fenerich[a], Juan Luiz Coelho-Silva[a], Priscila Santos Scheucher[a], Belinda Pinto Simões[a], Eduardo Magalhães Rego[a], Anne J. Ridley[b,c], João Agostinho Machado-Neto[a,1], Fabiola Traina[a,*]

[a] Department of Internal Medicine, University of Sao Paulo at Ribeirao Preto Medical School, Ribeirao Preto, Brazil
[b] Randall Centre for Cell and Molecular Biophysics, King's College London, London, United Kingdom
[c] School of Cellular and Molecular Medicine, University of Bristol, Bristol, United Kingdom

ARTICLE INFO

Keywords:
Acute lymphoblastic leukemia
NT157
IGF1R/IRS1
Cell signaling

ABSTRACT

The IGF1R/IRS1 signaling is activated in acute lymphoblastic leukemia (ALL) and can be targeted by the pharmacological inhibitors NT157 (IGF1R-IRS1/2 inhibitor) and OSI-906 (IGF1R/IR inhibitor). Here we investigate the cellular and molecular effects of NT157 and OSI-906 in ALL cells. NT157 and OSI-906 treatment reduced viability, proliferation and cell cycle progression in ALL cell lines. Similarly, in primary samples of patients with ALL, both OSI-906 and NT157 reduced viability, but only NT157 induced apoptosis. NT157 and OSI-906 did not show cytotoxicity in primary samples from healthy donor. NT157 and OSI-906 significantly decreased Jurkat cell migration, but did not modulate Namalwa migration. Consistent with the more potent effect of NT157 on cells, NT157 significantly modulated expression of 25 genes related to the MAPK signaling pathway in Jurkat cells, including oncogenes and tumor suppressor genes. Both compounds inhibited mTOR and p70S6K activity, but only NT157 inhibited AKT and 4-EBP1 activation. In summary, in ALL cells, NT157 has cytotoxic activity, whereas OSI-906 is cytostatic. NT157 has a stronger effect on ALL cells, and thus the direct inhibition of IRS1 may be a potential therapeutic target in ALL.

1. Introduction

Acute lymphoblastic leukemia (ALL) is an aggressive hematological malignancy that causes exacerbated lymphoblast proliferation (B or T cell origin) in the bone marrow, blood and tissues, and often signaling pathways are activated, which are important in the maintenance and progression of the disease [1,2]. The IGF1R signaling system contributes to the transformation and growth of malignant cells in neoplastic contexts [3,4], including in hematological malignancies [5]. IGF1R signaling enhances the ability of cancer cells to survive anchorage-independence, supporting tumor invasion and metastatic dissemination [5,6]. Binding of the IGF1 ligand to its transmembrane tyrosine kinase receptor IGF1R leads to tyrosine phosphorylation of its substrates IRS1 and IRS2 [7,8], which then recruit multiple proteins to transmit mitogenic, anti-apoptotic and anti-differentiation signals, mainly through the activation of the PI3K/AKT/mTOR and MAPK signaling pathways [9,10]. Recently, our group has identified *IRS1* as highly expressed in a cohort of 45 ALL patients in comparison with normal hematopoietic cells [11].

Several IGF1R inhibitors have been tested for effects on T- and B-cell leukemias. For example, the IGF1R inhibitors BMS-536924 and BMS-754807 decreased cell growth and reduced the survival of human T-ALL cell lines and primary T-ALL cells [12], similarly to PI3K/AKT/mTOR inhibitors [13,14]. The selective IGF1R inhibitor picropodophyllin (PPP) efficiently decreased cell viability, induced apoptosis, and G_2/M-phase cell cycle arrest in T-ALL [15] and diffuse large B-cell lymphoma [16]. OSI-906, a selective IGF1R and insulin receptor (IR) kinase inhibitor, reduced cell viability and induced apoptosis in primary cells from patients with chronic lymphoblastic leukemia [17], and acted synergistically with bortezomib to inhibit cell viability in multiple myeloma cell lines and primary patient cells [18]. NT157, a small molecule that leads to Ser-phosphorylation and subsequent degradation of IRS1 and IRS2, appears to be particularly promising in therapeutic strategies since it induces long-term inhibition of IGF1R-IRS1/2

* Corresponding author. Department of Internal Medicine, University of São Paulo at Ribeirão Preto Medical School, Av. Bandeirante 3900, Ribeirão Preto, SP, Brazil.
E-mail address: ftraina@fmrp.usp.br (F. Traina).
[1] Currently at Department of Pharmacology, Institute of Biomedical Sciences of the University of São Paulo, São Paulo, Brazil.

https://doi.org/10.1016/j.canlet.2019.04.030
Received 21 January 2019; Received in revised form 20 April 2019; Accepted 25 April 2019

signaling and it has been shown to be a powerful inhibitor of tumor cell growth in melanoma [19,20], prostate cancer [21], osteosarcoma [22] and colorectal cancer [23].

Despite the evidence that the IGF1R/IRS1 pathway contributes to the ALL phenotype, therapeutic strategies using IGF1R and/or IRS1 inhibitors have rarely been addressed for this disease. Here, we performed a preclinical characterization of the effects of NT157 and OSI-906 targeting IGF1R signaling in ALL cells.

2. Materials and methods

2.1. Cell culture and pharmacological inhibitors

Human acute lymphoblastic leukemia cell lines, Jurkat and MOLT-4 (T-ALL), and Namalwa and Raji (B-ALL), were obtained from ATCC (USA). Cells were authenticated [11] and were mycoplasma-free. NT157 was kindly provided by Prof. Alexander Levitzki [19] or it was obtained from Sun-Shinechem (CHN). OSI-906 was obtained from Selleckchem (USA). Both inhibitors were dissolved in DMSO (Sigma-Aldrich, USA) and stored as 10 mM stock solutions (final concentration of DMSO was less than 0.02% by volume).

2.2. MTT assay

Jurkat, MOLT-4, Namalwa, Raji and primary cells from healthy donors and ALL patients (1×10^4 cells/well) were cultured in 96-well plates in RPMI containing 10% FBS, in the presence of different doses of NT157 and OSI-906 or DMSO control for 24, 48 and 72 h. At the end of each culture period, 10 µL of a 5 mg/mL solution of methylthiazoletetrazolium (MTT) was added to each well followed by incubation at 37 °C for 4 h. The reaction was stopped using 100 µL of 0.1 N HCl in anhydrous isopropanol. Cell viability was evaluated by measuring the absorbance at 570 nm, using an iMark™ Microplate Absorbance Reader (Bio-Rad, USA). IC_{50} values were calculated using a nonlinear regression analysis and CalcuSyn software (Biosoft, USA).

2.3. Apoptosis assay

Jurkat, MOLT-4, Namalwa, Raji and primary cells from healthy donors and ALL patients (1×10^5 cells/well) were seeded in 24-well plates and treated with different doses of NT157 and OSI-906 or DMSO control for 24, 48 and 72 h. Cells were then washed twice with cold phosphate buffered saline (PBS) and resuspended in binding buffer containing 1 µg/mL propidium iodide (PI) and 1 µg/mL FITC- or APC-labeled Annexin V. After incubation for 15 min at room temperature in a light-protected area, specimens were analyzed by flow cytometry using the FACSCalibur (BD Bioscience, USA), followed by FlowJo software (Treestar, Inc., USA).

2.4. Assessment of cell proliferation by Ki-67 staining

Jurkat and Namalwa cells were treated with different doses of NT157 and OSI-906 or with DMSO control for 24 h, fixed with 70% ethanol and stored at −20 °C. Ki-67 staining was performed following the manufacturer's instructions (BD Bioscience) and the mean of fluorescence intensity (M.F.I.) was obtained by flow cytometry using the FACSCalibur. IgG isotype was used as negative control for each condition.

2.5. Cell cycle analysis

Cell cycle phases were determined using the BD Cycletest™ Plus DNA Reagent Kit (BD Bioscience) according to the manufacturer's instructions. Jurkat and Namalwa cells were cultured in the absence or presence of different doses of NT157 and OSI-906 for 24 h. DNA content distribution was analyzed with a FACSCalibur flow cytometer.

2.6. Western blotting analysis

Cells were lysed with extraction buffer (10 mM EDTA, 100 mM TRIS, 10 nM $Na_4P_2O_7$, 100 mM NaF, 10 mM Na_3VO_4, 2 mM phenylmethane sulfonyl fluoride, 1% Triton X-100). Equal amounts of protein were resolved by SDS-PAGE, then analyzed by western blotting with the indicated antibodies (Supplementary Table 1) and imaging using the SuperSignal™ West Dura Extended Duration Substrate System (Thermo Fisher Scientific, USA) and Gel Doc XR + system (Bio-Rad, USA). Cropped gels retain important bands, but whole gel images are available in Supplementary Fig. 1 and Supplementary Fig. 2.

2.7. MAPK signaling pathway profile by PCR array and quantitative PCR

Total RNA from Jurkat cells treated with 0.8 µM NT157 or DMSO control was obtained using TRIzol reagent (Thermo Fisher Scientific). The cDNA was synthesized from 1 µg of RNA using a High-Capacity cDNA Reverse Transcription Kit (Thermo Fisher Scientific). PCR array was performed using the Human MAP Kinase Signaling Pathway RT^2 Profiler PCR Array kit (SA Biosciences, USA). mRNA levels were normalized to those detected in untreated cells, and genes that presented a $\geq$ 2-fold change in any treatment were included in the heatmap using multiple experiment viewer (MeV) 4.9.0 software (http://mev.tm4.org). Amplification was performed in an ABI 7500 Sequence Detector System (Life technologies, USA). Quantitative PCR (qPCR) was performed with specific primers (Supplementary Table 2). The relative quantification value was calculated using the equation $2^{-\Delta\Delta CT}$.

2.8. Migration assay

Jurkat and Namalwa cells were cultured in RPMI containing 10% FBS, treated with 0.4 µM NT157 and 10 µM OSI-906 or DMSO control for 24 or 48 h, and 1×10^5 cells/well were seeded in 24-well plates previously coated with 10 µg/mL fibronectin (Sigma-Aldrich) for 2 h. Cell migration was followed by time-lapse microscopy using a Nikon Eclipse TE2000 microscope with a 10 × or 20 × objective and Metamorph software (Molecular Devices, UK). Images were acquired at 1 frame/1.45 min for 3 h for Jurkat and at 1 frame/5 min for 5 h for Namalwa cells at 37 °C, 5% CO_2. Cells in time-lapse movies were tracked using the Manual Tracking plugin of ImageJ software (http://rsb.info.nih.gov/ij). The mean accumulated distance traveled and cell velocity were determined from at least 30 cells for each condition in each of three independent experiments.

2.9. Primary cell culture

The Ethics Committee of the Institution approved this study and written informed consent was obtained from all subjects. Bone marrow or peripheral blood samples were collected from 10 ALL patients (median age 30 years [range 19–61]; 2 T-ALL and 8 B-ALL) (Supplementary Tables 3) and 4 healthy donors (median age 35 years [27–44]). Mononuclear cells were cultured in RPMI containing 30% FBS with antibiotics and recombinant cytokines (PeproTech, USA) (IL3 [30 ng/mL], IL7 [100 ng/mL], FLT3-ligand [100 ng/mL] and SCF [30 ng/mL]), at a confluence of 2×10^6 cells/mL. Cells were treated with different doses of NT157 and OSI-906 or DMSO control, and analyzed by MTT assay and annexin V/PI staining.

2.10. Statistical analysis

Statistical analyses were performed using GraphPad Prism 5 (GraphPad Software Inc., USA). Student's *t*-test or ANOVA test and Bonferroni post-test were used, as appropriate; $p < 0.05$ was considered as statistically significant.

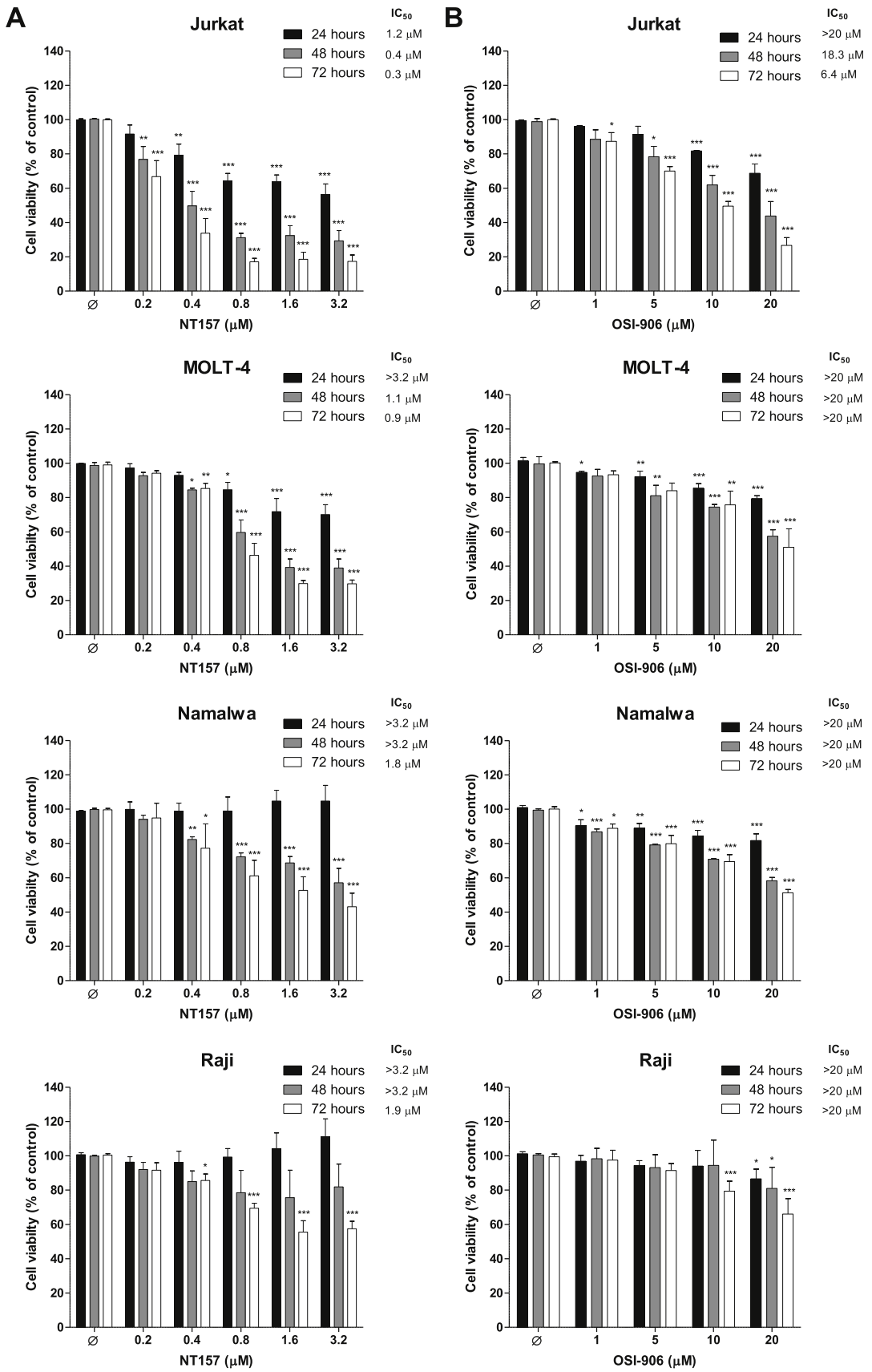

Fig. 1. NT157 (IGF1R/IRS1 inhibitor) and OSI-906 (IGF1R/IR inhibitor) reduce cell viability in ALL cell lines. Cell viability was determined by methylthiazoletetrazolium (MTT) assay for Jurkat, MOLT-4, Namalwa and Raji cells treated with **(A)** NT157 (0.2, 0.4, 0.8, 1.6 and 3.2 μM) and **(B)** OSI-906 (1, 5, 10 and 20 μM) for 24, 48 and 72 h and normalized to corresponding untreated control cells. Bar graphs represent the mean ± SD of at least three independent experiments. The *p* values and cell lines are indicated in the graphs. $*p < 0.05$, $**p < 0.01$ and $***p < 0.001$ for NT157-or OSI-906-treated cells *vs.* untreated cells; ANOVA test and Bonferroni post-test.

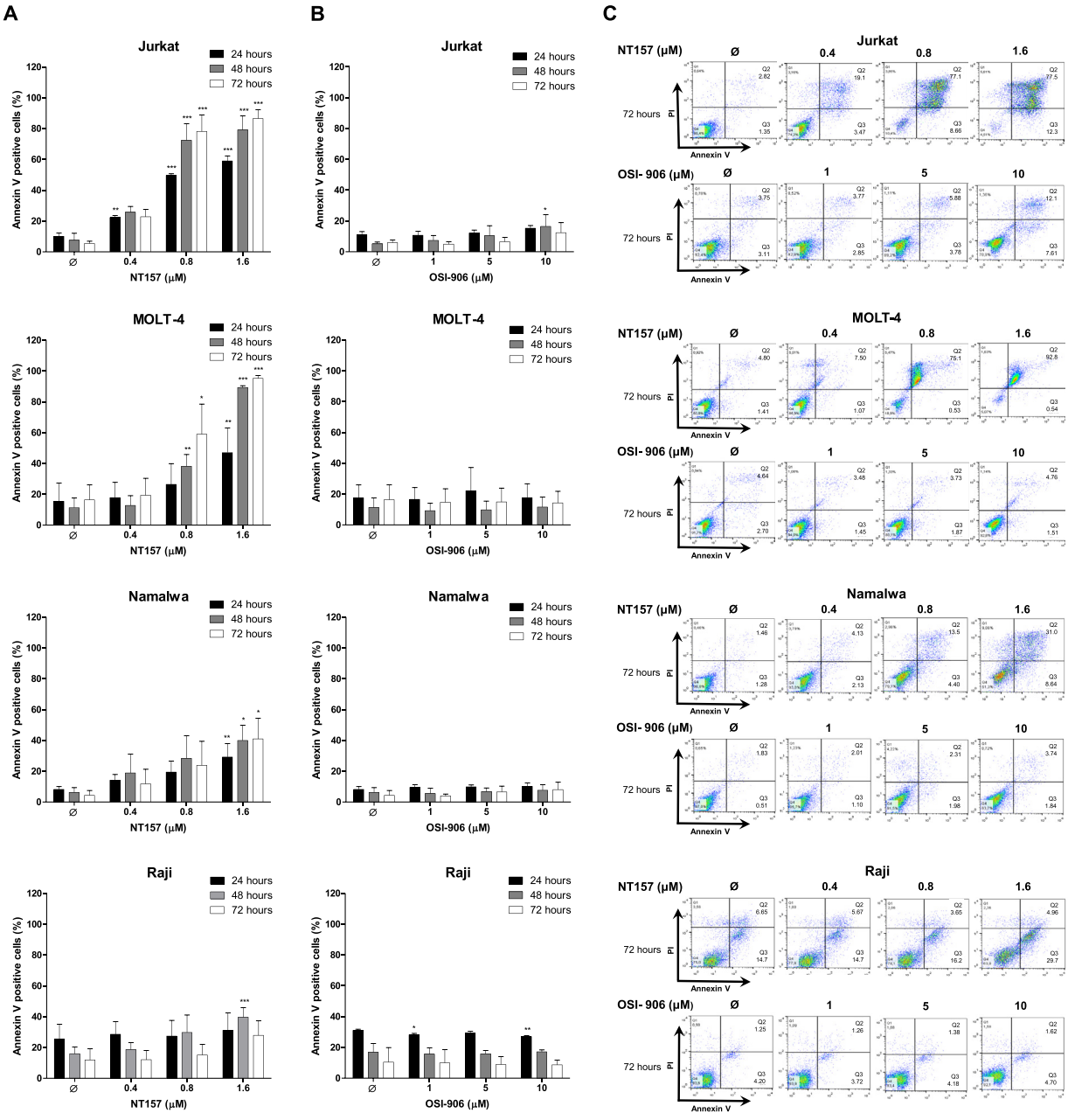

(caption on next page)

Fig. 2. NT157 (IGF1R/IRS1 inhibitor), but not OSI-906 (IGF1R/IR inhibitor), induces apoptosis in ALL cell lines. Apoptosis was detected by flow cytometry in Jurkat, MOLT-4, Namalwa and Raji cells treated with **(A)** NT157 (0.4, 0.8 and 1.6 μM) and **(B)** OSI-906 (1, 5 and 10 μM) or with DMSO vehicle control for 24, 48 and 72 h using an Annexin V/PI staining method. Bar graphs represent the mean ± SD of at least three independent experiments. The *p* values and cell lines are indicated in the graphs. $*p < 0.05$, $**p < 0.01$ and $***p < 0.001$ for NT157-or OSI-906-treated cells *vs.* untreated control cells; ANOVA test and Bonferroni post-test. **(C)** Representative dot plots are shown for each cell lineage for 72 h of NT157 or OSI-906 treatment compared to respective untreated cells; the upper and lower right quadrants cumulatively contain the apoptotic population (Annexin V positive cells). **(D)** Western blotting analysis for caspase 3 (total and cleaved) levels in total cell extracts from Jurkat, MOLT-4, Namalwa and Raji cells treated for 48 h with the indicated concentrations of NT157 or OSI-906. Membranes were reprobed with actin antibodies as a loading control.

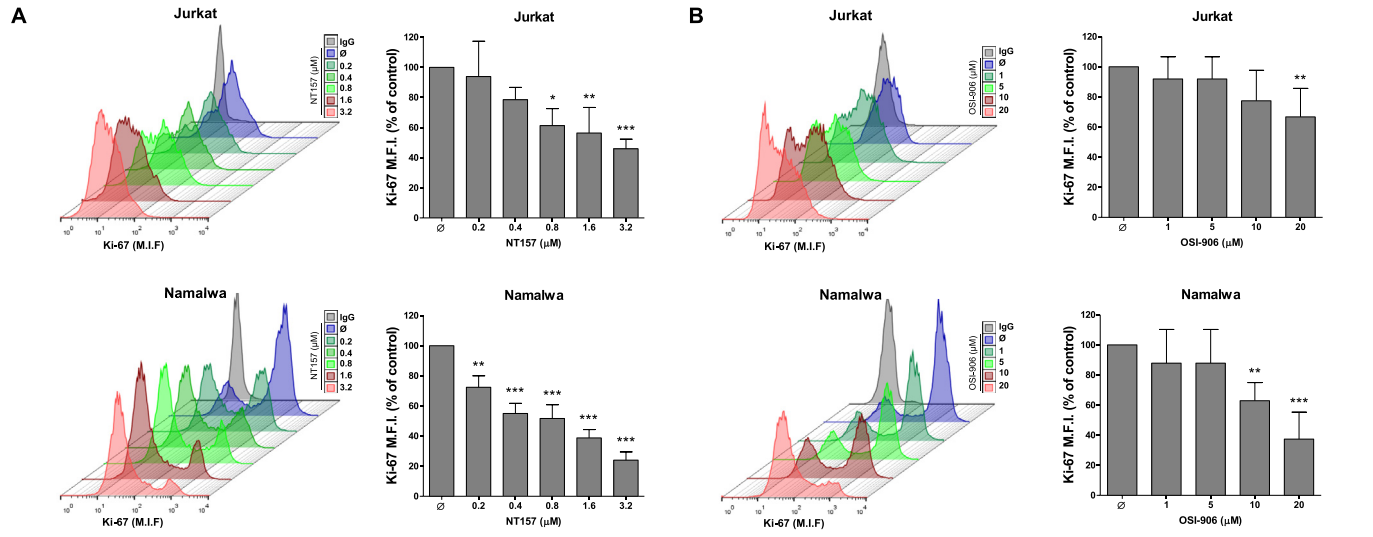

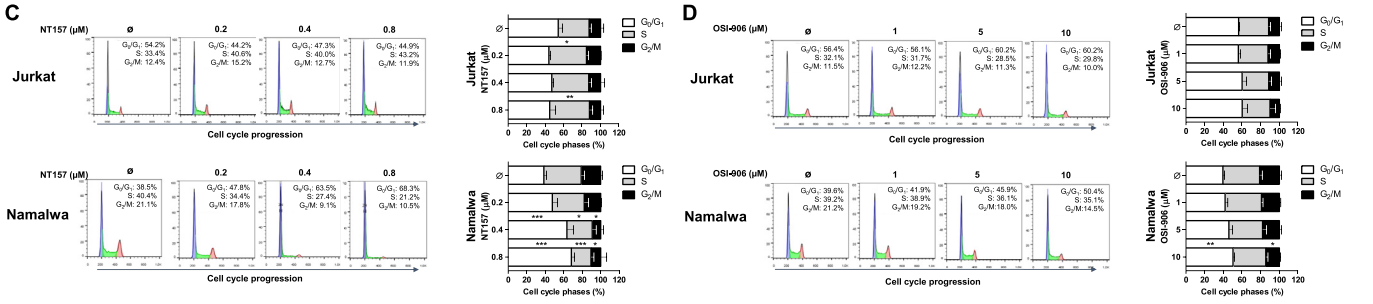

Fig. 3. NT157 and OSI-906 reduce cell proliferation and delay cell cycle progression in Jurkat and Namalwa cell lines. Ki-67 mean fluorescence intensity (M.F.I.) was determined by flow cytometry after incubation of Jurkat and Namalwa cells treated with **(A)** NT157 (0.2, 0.4, 0.8, 1.6 and 3.2 μM) and **(B)** OSI-906 (1, 5, 10 and 20 μM) for 24 h; histogram traces are illustrated. The bar graphs represent the Ki-67 M.F.I normalized to the respective untreated control cells, and the results are shown as mean ± SD of at least three independent experiments; $*p < 0.05$, $**p < 0.01$ and $***p < 0.001$, ANOVA test and Bonferroni post-test. **(C–D)** Cell cycle progression was determined in Jurkat or Namalwa cells treated with the indicated concentrations of **(C)** NT157 and **(D)** OSI-906 for 24 h. A representative histogram for each condition is illustrated. Bar graphs represent the mean ± SD of the percentage of cells in G_0/G_1, S and G_2/M phases after respective treatment for 24 h from at least three independent experiments. The *p* values and cell lines are indicated in the graphs. $*p < 0.05$, $**p < 0.01$ and $***p < 0.001$ for NT157-or OSI-906-treated cells *vs.* untreated cells; ANOVA test and Bonferroni post-test.

3. Results

3.1. IGF1R-IRS1/2 and IGF1R/IR inhibitors reduce cell number, proliferation and migration in ALL cell lines

To investigate the role of IGF signaling in ALL cells, we tested the effects of the IGF1R-IRS1/2 inhibitor NT157 and the IGF1R/IR inhibitor OSI-906. Both inhibitors significantly reduced MTT staining (a measure of cell metabolic activity that reflects in part the number of viable cells) in the T-ALL cell lines Jurkat and MOLT-4 and the B-ALL cell lines Namalwa and Raji. The effects on MTT staining increased at 48 and 72 h compared to 24 h and were dose-dependent (Fig. 1A–B). The IC_{50} values are indicated in Fig. 1.

We tested whether the effects of the two inhibitors in reducing MTT staining were due to apoptosis. NT157, but not OSI-906, significantly induced apoptosis in the ALL cell lines in a dose- and time-dependent manner (Fig. 2A–C). Consistent with these observations, only NT157 induced Caspase 3 cleavage in all ALL cell lines, with a stronger effect in Jurkat and MOLT-4 T-ALL cells (Fig. 2D).

Based on the results of MTT and apoptosis assays, Jurkat and Namalwa cell lines were selected for further investigation of the effects of IGF1R signaling inhibitors. Ki-67 analysis revealed that NT157 significantly reduced cell proliferation in Jurkat or Namalwa cells at all doses tested (Fig. 3A). OSI-906 treatment reduced cell proliferation in both cell types, but only at higher doses ($p \leq 0.05$) (Fig. 3B). NT157 was able to delay cell cycle progression, causing S-phase and G_0/G_1-phase arrest in Jurkat and Namalwa cells, respectively ($p \leq 0.05$) (Fig. 3C). OSI-906 induced cell cycle delay in G_0/G_1-phase only in Namalwa cells ($p \leq 0.05$) (Fig. 3D). Taken together, these results indicate that IGFR1 signaling inhibitors are cytostatic, inhibiting cell cycle progression, and can also be cytotoxic, inducing apoptosis.

To determine whether IGFR1 signaling inhibitors affected other

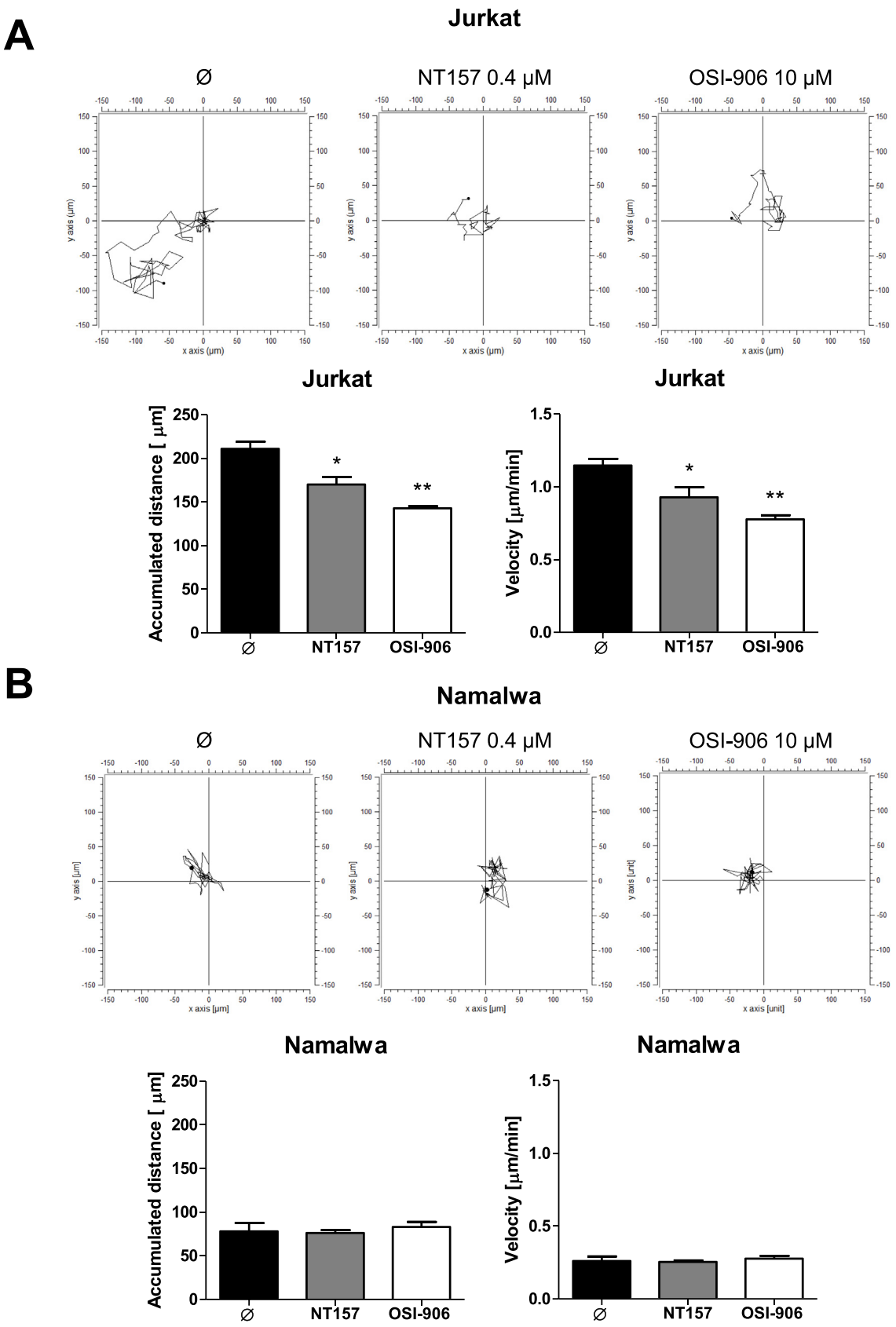

Fig. 4. NT157 and OSI-906 decrease Jurkat cell migration. Illustrative cell migration plot diagram of a single Jurkat (A) or Namalwa cell (B) treated with NT157 (0.4 μM), OSI-906 (10 μM) or vehicle (Ø). Images were obtained in a Nikon Eclipse TE2000 microscopy and analyzed with Manual tracking plugin in ImageJ software. The start point of each track was normalized to x = 0 and y = 0. Bar graphs represent the mean ± SD of accumulated distance traveled and cell velocity determined from at least 30 cells for each condition in each of three independent experiments after 24 and 48 h for Jurkat and Namalwa, respectively. The p values and cell lines are indicated in the graphs. *$p < 0.05$ and **$p < 0.01$ for NT157-or OSI-906-treated cells vs. vehicle-treated cells; ANOVA test with Bonferroni post-test.

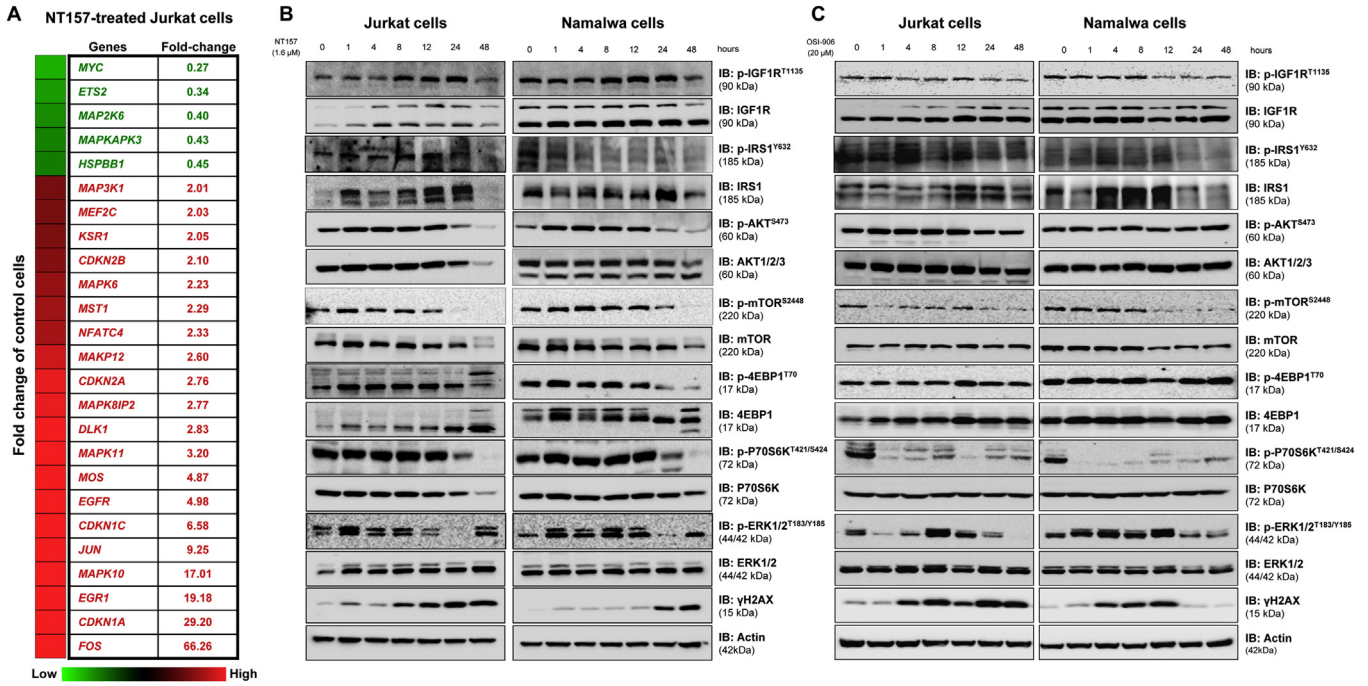

Fig. 5. NT157 and OSI-906 modulate PI3K/AKT/mTOR and MAPK signaling in Jurkat and Namalwa cell lines. (A) Gene expression heat map from qPCR array analysis of Jurkat cells treated with 0.8 μM NT157 for 24 h mRNA levels are normalized to those of untreated Jurkat cells and calculated as fold change in expression; genes demonstrating ≥2.0-fold in either direction compared to untreated cells in any treatment are included in the heat map. Two independent experiments of each condition were used for the analysis; green indicates repressed mRNA levels and red elevated mRNA levels. **(B–C)** Western blots for the indicated proteins and phospho-proteins in total cell extracts from Jurkat and Namalwa cells treated with (B) 1.6 μM NT157 and **(C)** 10 μM OSI-906. Membranes were reprobed with antibodies to actin as a loading control. (For interpretation of the references to color in this figure legend, the reader is referred to the Web version of this article.)

properties of ALL cells in addition to cell proliferation, we tested whether they affected cell migration using time-lapse microscopy. Both inhibitors significantly reduced the accumulated distance traveled and the velocity of Jurkat cells ($p \leq 0.05$) (Fig. 4A), but did not modulate the migration in Namalwa cells (Fig. 4B). This indicates that the effects of IGF1R signaling on cell migration are cell-type dependent, possibly reflecting differences in the spectrum of genetic mutations between Jurkat and Namalwa cells.

3.2. NT157 and OSI-906 modulate PI3K/AKT/mTOR and MAPK signaling in ALL cells

To investigate the molecular basis of the effects of IGF1R signaling inhibitors on cell cycle progression, we tested their effects on expression of MAPK-regulated genes using a PCR array. The expression of 25 genes increased or decreased ≥2-fold in NT157-treated Jurkat cells compared to DMSO-treated control cells: 20 were downregulated and 5 were upregulated genes (Fig. 5A; Supplementary Table 4). Based on the results of our functional experiments, we choose four genes (*CDKN1A, MYC, FOS* and *JUN*) involved in cell proliferation, apoptosis and cell cycle to validate by qPCR or western blotting using all 4 ALL cell lines. Increased expression of *CDKN1A*, *FOS* and *JUN* were induced by treatment with NT157 in the PCR array and this was confirmed by qPCR in all the cell lines tested ($p < 0.05$), except the *FOS* gene in Raji cells (Supplementary Fig. 3A). OSI-906 treatment significantly increased *FOS* expression in all the cell lines studied. However, OSI-906 induced a significant increase in *CDKN1A* and *JUN* expression only in Raji and Jurkat cells (Supplementary Fig. 3B). Western blotting analysis confirmed *MYC* downregulation in Jurkat and Namalwa cells after treatment with NT157 and OSI-906 (Supplementary Fig. 3C).

Both inhibitors reduced IRS1 tyrosine phosphorylation, as expected. We then tested the effects of the inhibitors on IGF1R-activated signaling pathways [5]. NT157 and OSI-906 inhibited mTOR and p706SK phosphorylation, but only NT157 inhibited AKT and 4-EBP1 phosphorylation. OSI-906 inhibited ERK, but NT157 induced ERK activation, followed by inhibition and re-activation from a lower to higher time of exposure to the compound. NT157 and OSI-906 increased γH2A.X expression, a marker of DNA damage [24,25] (Fig. 5B–C). Taken together, these results indicated that the two inhibitors reduce activity of IGF1-activated signaling pathways in ALL cells, including expression of MYC, which is known to be important for cell growth and proliferation [26,27].

3.3. NT157 and OSI-906 reduce cell viability in primary ALL samples, but not in normal leukocytes

We tested whether the effects we observed on ALL cell lines were also observed in primary ALL cells from patients. In B-ALL primary cells, NT157 induced a significant decrease in MTT staining and an increase in apoptosis, whereas OSI-906 significantly decreased MTT staining, but did not modulate apoptosis (Fig. 6A). In normal peripheral blood mononuclear cells from four different donors, neither NT157 nor OSI-906 modulated MTT staining or apoptosis at any dose tested (Fig. 6B).

4. Discussion

We have investigated the effects of two IGF1R signaling inhibitors, NT157 and OSI-906, in ALL cellular models. Our results demonstrate that NT157 has a stronger effect on cells: it reduced cell viability, proliferation, cell cycle progression and induced apoptosis in ALL cells, whereas OSI-906 had a weaker effect on cell viability, proliferation and cell cycle progression, and did not induce apoptosis. These effects were observed in the absence of added IGF1, indicating that IGF1R signaling is constitutively activated in ALL cells.

At the molecular level, NT157 reduced IRS1 protein levels and reduced the activity of signaling components activated downstream of IRS1, including AKT, mTOR and P70S6K. It also increased the

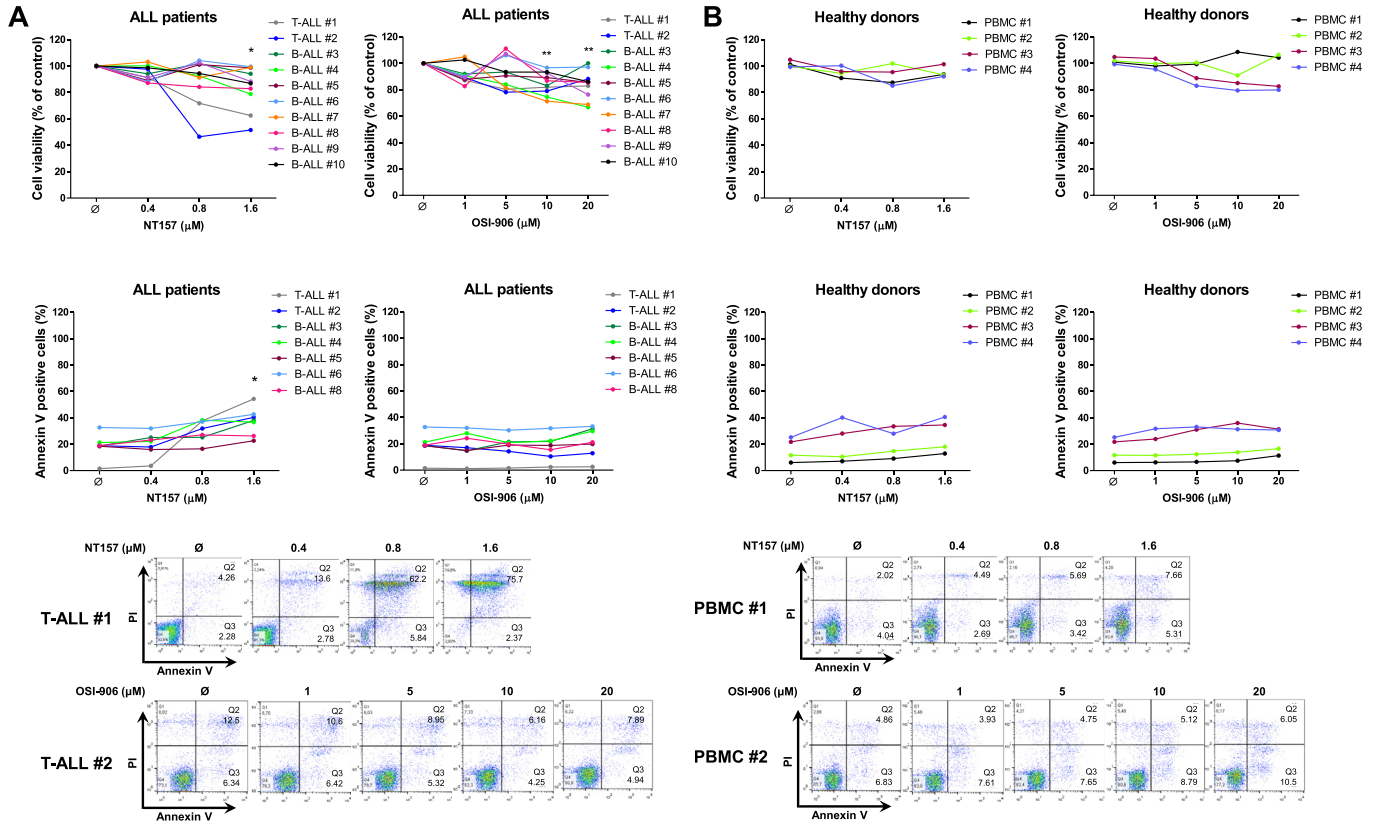

Fig. 6. NT157 and OSI-906 reduce cell viability in primary ALL cells, but not in normal hematopoietic cells. Peripheral blood or bone marrow mononuclear cells from ALL patients **(A)** and peripheral blood mononuclear cells (PBMC) from healthy donors **(B)** were treated, or not, with NT157 (0.4, 0.8 and 1.6 μM) and/or OSI-906 (1, 5, 10 and 20 μM) for 72 h. Cell viability was determined by methylthiazoletetrazolium (MTT) assay and apoptosis was detected by flow cytometry using an annexin V/PI staining method. The lines in the graphs represent primary cells from each ALL patient or normal PBMC sample. Representative dot plots of primary cells from one ALL patient and one normal PBMC sample are shown; the upper and lower right quadrants cumulatively contain the apoptotic population (annexin V positive cells). The *p* values are indicated in the graphs; $*p < 0.05$ and $**p < 0.01$ for NTS157- and/or OSI-906-treated cells *vs.* untreated cells; ANOVA test and Bonferroni post-test.

phosphorylated form of a histone variant H2A.X at Ser139, γH2A.X, and *CDKN1A* expression in Jurkat and Namalwa cells. γH2A.X a well-accepted DNA damage marker, which recruits DNA repair protein complexes that then activate *CDKN1A* expression (encoding p21) leading to cell cycle arrest [24,25]. It is well established that p21 mediates cell growth arrest and apoptosis under a variety of cellular stress [28–31], which corroborates with our findings that NT157 induces apoptosis in ALL cells. Furthermore, NT157 increased *JUN* and *FOS* expression, which are AP-1 transcription factor subunits that are activated by cellular stress, balancing survival and apoptosis processes [32,33]. Recently, proteomic analysis of melanoma cell lines treated with NT157 revealed an increased activation of stress-related kinases, JNK and p38 MAPK [34], in agreement with our observations that NT157 induces cellular stress in ALL cells.

Among the mechanisms of action of NT157, one is the degradation of IRS proteins mediated by activation and phosphorylation of ERK [19]. In fact, our results indicated a transient increase in ERK activity in the first hours of NT157 treatment, followed by a consistent reduction in IRS1 expression, and a later inhibition of ERK, suggesting that the proposed mechanism of NT157 action in melanoma cells [19] is preserved in ALL models. This transient ERK modulation may be secondary to a regulatory loop that is similar to that described for insulin action [35]. The increase in the expression of the AP-1 subunits *FOS* and *JUN*, and possibly JNK activity, suggests another mechanism of IRS1 protein regulation by NT517, since JNK can phosphorylate IRS proteins and prevent their interaction with insulin receptor [35].

OSI-906 has been reported to have excellent pre-clinical results with anti-proliferative effects in a variety of cancer cell lines *in vitro* and in an IGF1R-drived xenograft model *in vivo* [36]. However, we observe that OS1-906 is less potent than NT157 in its effects on ALL cell proliferation and survival. The differences we observe between the effects of the two inhibitors are likely to reflect their distinct mechanisms of action. NT157 inhibits the cytoplasmic IRS1/2 adaptor proteins [19], and other signaling pathways or receptors that depend on IRS1/2 proteins, producing an amplification effect. On the other hand, OSI-906 inhibits cell signaling selectively from IGF1R and IR [36], which may allow cells to activate downstream pathways via other receptors. One such example is the maintenance of AKT activation in ALL cells following OSI-906 treatment, but not NT157. AKT is known to protect cells from apoptosis. For example, AKT phosphorylates and inhibits BAD, which is a key BCL2 family protein involved in the induction of apoptosis [37–39]. Thus, in the light of our results, further investigation combining OSI-906 and AKT selective inhibitors in ALL models may be of interest. We have previously demonstrated that the IGF1R/IRS1 axis plays a role in MYC expression, which was an independent prognostic factor in the ALL cohort analyzed [11]. We confirm here that both NT157 and OSI-906 reduce MYC expression, which may contribute to their effects in reducing cell cycle progression and survival [26,27].

It is remarkable that both T-ALL cell lines and primary patient T-ALL samples had a stronger response to the two inhibitors, especially to NT157, than the B-ALL cells and B-ALL patient samples. Similarly, NT157 inhibited Jurkat (T-ALL), but not Namalwa (B-ALL) cell migration. More importantly, both drugs showed selectivity for malignant lymphocytes, since no cytotoxicity was observed for lymphocytes from healthy donors, which express low levels of IGF1R and IRS1 expression [11]. Similar results were reported in the melanoma models: NT157

reduced the viability of melanoma cells, but not of normal melanocytes [19]. Based on these findings, NT157 may be an interesting inhibitor of IGF1R/IRS signaling in the context of ALL, since this drug has greater potency compared to OSI-906, it acts more quickly and potentially preserves the therapeutic index (selectivity against primary leukemia cells).

In summary, NT157 exerts cytotoxic activities, while OSI-906 induces cytostatic effects as evidenced by G_0/G_1 cell cycle arrest, and did not affect apoptosis in ALL cells. We identify differences in the molecular effects of the two inhibitors, including evidence that AKT inhibition and DNA damage responses are selectively induced by NT157, explaining its ability to induce apoptosis. Our results indicate that pharmacological inhibition of IRS1 is a potential new treatment for ALL.

Conflict of interest disclosure

The authors declare no potential conflicts of interests.

Acknowledgments

Funding for this work was supported by São Paulo Research Foundation (FAPESP), Grants #2014/14844-9, #14/50947-7, #13/08135-2, Coordination for the Improvement of Higher Education Personnel (CAPES), National Council for Scientific and Technological Development (CNPq), and Cancer Research UK, Grant No. C6620/A15961.

Appendix A. Supplementary data

Supplementary data to this article can be found online at https://doi.org/10.1016/j.canlet.2019.04.030.

References

[1] C.H. Pui, M.V. Relling, J.R. Downing, Acute lymphoblastic leukemia, N. Engl. J. Med. 350 (2004) 1535–1548 https://doi.org/10.1056/NEJMra023001.
[2] H. Inaba, M. Greaves, C.G. Mullighan, Acute lymphoblastic leukaemia, Lancet 381 (2013) 1943–1955 https://doi.org/10.1016/S0140-6736(12)62187-4.
[3] M. Kaleko, W.J. Rutter, A.D. Miller, Overexpression of the human insulin like growth factor I receptor promotes ligand-dependent neoplastic transformation, Mol. Cell Biol. 10 (1990) 464–473.
[4] C. Sell, G. Dumenil, C. Deveaud, M. Miura, D. Coppola, T. DeAngelis, R. Rubin, A. Efstratiadis, R. Baserga, Effect of a null mutation of the insulin-like growth factor I receptor gene on growth and transformation of mouse embryo fibroblasts, Mol. Cell Biol. 14 (1994) 3604–3612.
[5] D. Vishwamitra, S.K. George, P. Shi, A.O. Kaseb, H.M. Amin, Type I insulin-like growth factor receptor signaling in hematological malignancies, Oncotarget 8 (2017) 1814–1844 https://doi.org/10.18632/oncotarget.12123.
[6] B. Himmelmann, C. Terry, B.R. Dey, W. Lopaczynski, P. Nissley, Anchorage-independent growth of fibroblasts that express a truncated IGF-I receptor, Biochem. Biophys. Res. Commun. 286 (2001) 472–477 https://doi.org/10.1006/bbrc.2001.5417.
[7] M.G. Myers Jr., X.J. Sun, B. Cheatham, B.R. Jachna, E.M. Glasheen, J.M. Backer, M.F. White, IRS-1 is a common element in insulin and insulin-like growth factor-I signaling to the phosphatidylinositol 3'-kinase, Endocrinology 132 (1993) 1421–1430 https://doi.org/10.1210/endo.132.4.8384986.
[8] R. Baserga, F. Peruzzi, K. Reiss, The IGF-1 receptor in cancer biology, Int. J. Cancer 107 (2003) 873–877 https://doi.org/10.1002/ijc.11487.
[9] D. Beitner-Johnson, V.A. Blakesley, Z. Shen-Orr, M. Jimenez, B. Stannard, L.M. Wang, J. Pierce, D. LeRoith, The proto-oncogene product c-Crk associates with insulin receptor substrate-1 and 4PS. Modulation by insulin growth factor-I (IGF) and enhanced IGF-I signaling, J. Biol. Chem. 271 (1996) 9287–9290.
[10] A. Virkamaki, K. Ueki, C.R. Kahn, Protein-protein interaction in insulin signaling and the molecular mechanisms of insulin resistance, J. Clin. Investig. 103 (1999) 931–943 https://doi.org/10.1172/JCI6609.
[11] J.C. Fernandes, A.P.N. Rodrigues Alves, J.A. Machado-Neto, R. Scopim-Ribeiro, B.A. Fenerich, F.B. da Silva, B.P. Simoes, E.M. Rego, F. Traina, IRS1/beta-Catenin Axis is activated and induces MYC expression in acute lymphoblastic leukemia cells, J. Cell. Biochem. 118 (2017) 1774–1781 https://doi.org/10.1002/jcb.25845.
[12] H. Medyouf, S. Gusscott, H. Wang, J.C. Tseng, C. Wai, O. Nemirovsky, A. Trumpp, F. Pflumio, J. Carboni, M. Gottardis, M. Pollak, A.L. Kung, J.C. Aster, M. Holzenberger, A.P. Weng, High-level IGF1R expression is required for leukemia-initiating cell activity in T-ALL and is supported by Notch signaling, J. Exp. Med. 208 (2011) 1809–1822 https://doi.org/10.1084/jem.20110121.
[13] R. Avellino, S. Romano, R. Parasole, R. Bisogni, A. Lamberti, V. Poggi, S. Venuta, M.F. Romano, Rapamycin stimulates apoptosis of childhood acute lymphoblastic leukemia cells, Blood 106 (2005) 1400–1406 https://doi.org/10.1182/blood-2005-03-0929.
[14] F. Chiarini, F. Fala, P.L. Tazzari, F. Ricci, A. Astolfi, A. Pession, P. Pagliaro, J.A. McCubrey, A.M. Martelli, Dual inhibition of class IA phosphatidylinositol 3-kinase and mammalian target of rapamycin as a new therapeutic option for T-cell acute lymphoblastic leukemia, Cancer Res. 69 (2009) 3520–3528 https://doi.org/10.1158/0008-5472.CAN-08-4884.
[15] Z. Huang, Z. Fang, H. Zhen, L. Zhou, H.M. Amin, P. Shi, Inhibition of type I insulin-like growth factor receptor tyrosine kinase by picropodophyllin induces apoptosis and cell cycle arrest in T lymphoblastic leukemia/lymphoma, Leuk. Lymphoma 55 (2014) 1876–1883 https://doi.org/10.3109/10428194.2013.862241.
[16] T. Stromberg, X. Feng, M. Delforoush, M. Berglund, Y. Lin, M. Axelson, O. Larsson, P. Georgii-Hemming, J. Lennartsson, G. Enblad, Picropodophyllin inhibits proliferation and survival of diffuse large B-cell lymphoma cells, Med. Oncol. 32 (2015) 188 https://doi.org/10.1007/s12032-015-0630-y.
[17] N. Yaktapour, R. Ubelhart, J. Schuler, K. Aumann, C. Dierks, M. Burger, D. Pfeifer, H. Jumaa, H. Veelken, T. Brummer, K. Zirlik, Insulin-like growth factor-1 receptor (IGF1R) as a novel target in chronic lymphocytic leukemia, Blood 122 (2013) 1621–1633 https://doi.org/10.1182/blood-2013-02-484386.
[18] D.J. Kuhn, Z. Berkova, R.J. Jones, R. Woessner, C.C. Bjorklund, W. Ma, R.E. Davis, P. Lin, H. Wang, T.L. Madden, C. Wei, V. Baladandayuthapani, M. Wang, S.K. Thomas, J.J. Shah, D.M. Weber, R.Z. Orlowski, Targeting the insulin-like growth factor-1 receptor to overcome bortezomib resistance in preclinical models of multiple myeloma, Blood 120 (2012) 3260–3270 https://doi.org/10.1182/blood-2011-10-386789.
[19] H. Reuveni, E. Flashner-Abramson, L. Steiner, K. Makedonski, R. Song, A. Shir, M. Herlyn, M. Bar-Eli, A. Levitzki, Therapeutic destruction of insulin receptor substrates for cancer treatment, Cancer Res. 73 (2013) 4383–4394 https://doi.org/10.1158/0008-5472.CAN-12-3385.
[20] E. Flashner-Abramson, S. Klein, G. Mullin, E. Shoshan, R. Song, A. Shir, Y. Langut, M. Bar-Eli, H. Reuveni, A. Levitzki, Targeting melanoma with NT157 by blocking Stat3 and IGF1R signaling, Oncogene 35 (2016) 2675–2680 https://doi.org/10.1038/onc.2015.229.
[21] N. Ibuki, M. Ghaffari, H. Reuveni, M. Pandey, L. Fazli, H. Azuma, M.E. Gleave, A. Levitzki, M.E. Cox, The tyrphostin NT157 suppresses insulin receptor substrates and augments therapeutic response of prostate cancer, Mol. Canc. Therapeut. 13 (2014) 2827–2839 https://doi.org/10.1158/1535-7163.MCT-13-0842.
[22] C. Garofalo, M. Capristo, C. Mancarella, H. Reunevi, P. Picci, K. Scotlandi, Preclinical effectiveness of selective inhibitor of IRS-1/2 NT157 in osteosarcoma cell lines, Front. Endocrinol. 6 (2015) 74 https://doi.org/10.3389/fendo.2015.00074.
[23] E. Sanchez-Lopez, E. Flashner-Abramson, S. Shalapour, Z. Zhong, K. Taniguchi, A. Levitzki, M. Karin, Targeting colorectal cancer via its microenvironment by inhibiting IGF-1 receptor-insulin receptor substrate and STAT3 signaling, Oncogene 35 (2016) 2634–2644 https://doi.org/10.1038/onc.2015.326.
[24] T. Abbas, A. Dutta, p21 in cancer: intricate networks and multiple activities, Nat. Rev. Canc. 9 (2009) 400–414 https://doi.org/10.1038/nrc2657.
[25] W.S. El-Deiry, p21(WAF1) mediates cell-cycle inhibition, relevant to cancer suppression and therapy, Cancer Res. 76 (2016) 5189–5191 https://doi.org/10.1158/0008-5472.CAN-16-2055.
[26] C.E. Nesbit, J.M. Tersak, E.V. Prochownik, MYC oncogenes and human neoplastic disease, Oncogene 18 (1999) 3004–3016 https://doi.org/10.1038/sj.onc.1202746.
[27] M. Schick, S. Habringer, J.A. Nilsson, U. Keller, Pathogenesis and therapeutic targeting of aberrant MYC expression in haematological cancers, Br. J. Haematol. 179 (2017) 724–738 https://doi.org/10.1111/bjh.14917.
[28] C. Deng, P. Zhang, J.W. Harper, S.J. Elledge, P. Leder, Mice lacking p21CIP1/WAF1 undergo normal development, but are defective in G1 checkpoint control, Cell 82 (1995) 675–684.
[29] W.S. el-Deiry, J.W. Harper, P.M. O'Connor, V.E. Velculescu, C.E. Canman, J. Jackman, J.A. Pietenpol, M. Burrell, D.E. Hill, Y. Wang, et al., WAF1/CIP1 is induced in p53-mediated G1 arrest and apoptosis, Cancer Res. 54 (1994) 1169–1174.
[30] A.L. Gartel, A.L. Tyner, The role of the cyclin-dependent kinase inhibitor p21 in apoptosis, Mol. Canc. Therapeut. 1 (2002) 639–649.
[31] Y. Zhang, N. Fujita, T. Tsuruo, Caspase-mediated cleavage of p21Waf1/Cip1 converts cancer cells from growth arrest to undergoing apoptosis, Oncogene 18 (1999) 1131–1138 https://doi.org/10.1038/sj.onc.1202426.
[32] P. Angel, M. Karin, The role of Jun, Fos and the AP-1 complex in cell-proliferation and transformation, Biochim. Biophys. Acta 1072 (1991) 129–157.
[33] Y.T. Ip, R.J. Davis, Signal transduction by the c-Jun N-terminal kinase (JNK)–from inflammation to development, Curr. Opin. Cell Biol. 10 (1998) 205–219.
[34] S.P. Su, E. Flashner-Abramson, S. Klein, M. Gal, R.S. Lee, J. Wu, A. Levitzki, R.J. Daly, Impact of the anticancer drug NT157 on tyrosine kinase signaling networks, Mol. Canc. Therapeut. 17 (2018) 931–942 https://doi.org/10.1158/1535-7163.MCT-17-0377.
[35] V. Aguirre, E.D. Werner, J. Giraud, Y.H. Lee, S.E. Shoelson, M.F. White, Phosphorylation of Ser307 in insulin receptor substrate-1 blocks interactions with the insulin receptor and inhibits insulin action, J. Biol. Chem. 277 (2002) 1531–1537 https://doi.org/10.1074/jbc.M101521200.
[36] M.J. Mulvihill, A. Cooke, M. Rosenfeld-Franklin, E. Buck, K. Foreman, D. Landfair, M. O'Connor, C. Pirritt, Y. Sun, Y. Yao, L.D. Arnold, N.W. Gibson, Q.S. Ji, Discovery of OSI-906: a selective and orally efficacious dual inhibitor of the IGF-1 receptor and insulin receptor, Future Med. Chem. 1 (2009) 1153–1171 https://doi.org/10.4155/fmc.09.89.

[37] S. Zhao, M. Konopleva, M. Cabreira-Hansen, Z. Xie, W. Hu, M. Milella, Z. Estrov, G.B. Mills, M. Andreeff, Inhibition of phosphatidylinositol 3-kinase dephosphorylates BAD and promotes apoptosis in myeloid leukemias, Leukemia 18 (2004) 267–275 https://doi.org/10.1038/sj.leu.2403220.

[38] B.C. Bornhauser, L. Bonapace, D. Lindholm, R. Martinez, G. Cario, M. Schrappe, F.K. Niggli, B.W. Schafer, J.P. Bourquin, Low-dose arsenic trioxide sensitizes glucocorticoid-resistant acute lymphoblastic leukemia cells to dexamethasone via an Akt-dependent pathway, Blood 110 (2007) 2084–2091 https://doi.org/10.1182/blood-2006-12-060970.

[39] S.R. Datta, H. Dudek, X. Tao, S. Masters, H. Fu, Y. Gotoh, M.E. Greenberg, Akt phosphorylation of BAD couples survival signals to the cell-intrinsic death machinery, Cell 91 (1997) 231–241.